



Studying of COVID-19 fractional model: Stability analysis

Sanaa L. Khalaf*, Mohammed S. Kadhim, Ayad R. Khudair

Department of Mathematics, College of Science, University of Basrah, Basrah, Iraq



ARTICLE INFO

Keywords:

COVID-19
Mathematical models
Caputo fractional derivative
Sensitivity analyses
Stability analysis
Ulam–Hyers stability
Fractional Euler method

ABSTRACT

This article focuses on the recent epidemic caused by COVID-19 and takes into account several measures that have been taken by governments, including complete closure, media coverage, and attention to public hygiene. It is well known that mathematical models in epidemiology have helped determine the best strategies for disease control. This motivates us to construct a fractional mathematical model that includes quarantine categories as well as government sanctions. In this article, we prove the existence and uniqueness of positive bounded solutions for the suggested model. Also, we investigate the stability of the disease-free and endemic equilibriums by using the basic reproduction number (BRN). Moreover, we investigate the stability of the considering model in the sense of Ulam–Hyers criteria. To underpin and demonstrate this study, we provide a numerical simulation, whose results are consistent with the analysis presented in this article.

1. Introduction

To combat the spread of COVID-19, all governments around the world have made significant efforts and taken preventive measures.^{1–3} In Wuhan, the capital of Hubei province, China, COVID-19 was first detected which is a new strain of SARS-CoV-2.^{4,5} In the months following its discovery, the number of patients grew at an exponential rate. According to the World Health Organization's situation report, there were 5 304 772 total cases and 342 029 deaths worldwide as of May 25, 2020. The use of mathematical models in epidemics is very important for understanding the nature of these epidemics as well as for designing effective strategies for controlling them.^{6–8} As a contribution from some mathematicians to reduce the COVID-19 pandemic, many researchers have adopted the development of models for this emerging epidemic. Where some researchers took from developing some models of the spread of epidemics such as SEIR and SIR to design a model that simulates the spread of Corona disease.^{9–19} The COVID-19 severity was calculated by Wu et al. using the dynamics of transition in Ref. 20. There have been investigations into random transition models in Refs. 21, 22. The general multi-group SEIRA model for modeling COVID-19 diffusion in a heterogeneous population was represented and numerically tested in Ref. 23. Differential equations in their various forms (ordinary, randomly detected, partial, fractional, or with delay) are an essential mathematical tool for modeling many epidemics.⁸ Many research attempts have been made to prevent epidemic outbreaks via optimum control.^{24–26} Mathematical studies of epidemic illnesses have become more relevant.^{27–29} Several studies have been introduced to control HIV,³⁰ dengue fever,³¹ TB,³² SIR,^{33,34} and SIRS.³⁵

Fractional differential equations (FDEs) provided an accurate description of the dynamics of epidemiological models,³⁶ taking into

account information about a population's memory and learning mechanisms, which influence disease spread. In this paper, we used a fractional mathematical model that includes the quarantine category and methods taken by the government to prevent the spread of disease and demonstrated the existence of non-negative and bounded solutions.

Many authors prefer to use FDEs to describe epidemic models since they carry more memory information and provide a learning mechanism for the spread of disease in the population compared to the ordinary differential equation, which is incapable of serving this purpose. Also, the region of stability for the FDEs is larger than that for the ordinary differential equations. Furthermore, the fractional derivative is a non-local operator, whereas the classical derivative is a local operator. In other words, the description of epidemic models by using fractional differential equations takes into account all historical and current states, which makes them more realistic and more general in nature.^{37,38} This prompted us to develop the Caputo fractional mathematical model for COVID-19 and introduce details about the existence of a unique positive solution and its behavior. In spite of the fact that there are many definitions of a fractional derivative, many scholars prefer to use the Caputo derivative to describe mathematical models by means of FDEs. In fact, due to the initial conditions of FDEs with Caputo derivatives containing integer order derivatives with physical meanings like distance, speed, and acceleration, FDEs with Caputo derivatives are widely used in real-world applications.³⁹

* Corresponding author.

E-mail addresses: sanaasanaa1978@yahoo.com (S.L. Khalaf), mohammedsari@yahoo.com (M.S. Kadhim), ayadayad1970@yahoo.com (A.R. Khudair).

2. Fundamentals of fractional calculus

In this part, we will present some related material about FDE, including the Riemann–Liouville fractional (R-LF) integral, Caputo fractional derivative definition, the existence, and uniqueness of FDE solutions, as well as some key properties and theorems in the field of stability analysis.

Definition 2.1 (Ref. 40). The left and right R-LF integral of order $\alpha > 0$ of f are given by

$${}_a J_t^\alpha f(t) = \frac{1}{\Gamma(\alpha)} \int_a^t (t-\xi)^{\alpha-1} f(\xi) d\xi, \quad (2.1)$$

$${}_t J_b^\alpha f(t) = \frac{1}{\Gamma(\alpha)} \int_t^b (\xi-t)^{\alpha-1} f(\xi) d\xi, \quad (2.2)$$

respectively.

Definition 2.2 (Ref. 40). The right (left) Caputo fractional derivative of order $m-1 < \alpha < m$, $m \in \mathbb{Z}_+$ are defined as follows:

$${}_t^C D_t^\alpha y(t) = \frac{(-1)^m}{\Gamma(m-\alpha)} \int_t^b (\xi-t)^{m-\alpha-1} y^{(m)}(\xi) d\xi, \quad (2.3)$$

$${}_a^C D_t^\alpha y(t) = \frac{1}{\Gamma(m-\alpha)} \int_a^t (t-\xi)^{m-\alpha-1} y^{(m)}(\xi) d\xi. \quad (2.4)$$

Lemma 2.1 (Ref. 41). If $g(t, y^*) = 0$, then the Caputo FDE

$$\begin{aligned} {}_{t_0}^C D_t^\alpha y(t) &= g(t, y(t)) \\ y(t_0) &= y_0 \end{aligned} \quad (2.5)$$

with $0 < \alpha \leq 1$ has equilibrium point at y^* .

Theorem 2.1 (Ref. 42). Consider y^* be an equilibrium point of the Caputo FDE (2.5), if $|\arg(\lambda)| > \frac{\alpha\pi}{2}$ holds for all λ , where λ is the Jacobian matrix of $g(t, y(t)) = 0$ at y^* , then y^* is locally asymptotically stable.

Definition 2.3. If $F(s)$ be Laplace transform of $F(t)$, then

$$L\{{}_{a}^C D_t^\alpha F(t), s\} = s^\alpha F(s) - \sum_{i=0}^{m-1} s^{\alpha-i-1} F^{(i)}(0), \quad \alpha \in (m-1, m), \quad m \in \mathbb{Z}_+ \quad (2.6)$$

Theorem 2.2 (Ref. 40). Let $g(t, y(t)) : \mathbb{R} \times \mathbb{R}^n \rightarrow \mathbb{R}$ be a continuous function with respect y and Lebesgue measurable with respect to t . If there are two positive constants γ and μ such that $\|g(t, y(t))\| \leq \mu + \gamma \|y(t)\|$ satisfy $\forall (t, y) \in \mathbb{R} \times \mathbb{R}^n$, then there is a solution to the Caputo FDE (2.5) started from the point (t_0, y_0) .

Lemma 2.2 (Ref. 40). Suppose that all conditions in Theorem 2.2 hold and $\frac{\partial g(t, y(t))}{\partial y(t)}$ is continuous with respect y , then the solution of the Caputo FDE (2.5) is unique.

Definition 2.4. The function $E_{r,n}(t)$ for $t \in \mathbb{R}$ is defined by

$$E_{r,n}(t) = \sum_{i=0}^{\infty} \frac{t^i}{\Gamma(r i + n)}, \quad r, n > 0 \quad (2.7)$$

where $E_{r,n}(t)$ is called the generalized Mittag-Leffler function and satisfies

$$\begin{aligned} E_{r,n}(t) &= \frac{1}{\Gamma(n)} + t E_{r,r+n}(t), \quad n, r > 0 \\ L\{t^{n-1} E_{r,n}(\pm \rho t^r)\} &= \frac{s^{r-n}}{s^r \mp \rho} \end{aligned}$$

where L is the Laplace transform.

Table 1
Represent variables for COVID-19 fractional model.

Model symbols	Symptoms of a disease
S	Susceptible population fraction.
E	Exposed population fraction.
I	Hospitalized infected population fraction.
Q	The population that is quarantined.
R	Recovered or Removed population fraction.

Table 2
Represent parameters for COVID-19 fractional model.

Parameters	Description
A	Recruitment in its entirety
ϑ_1	The contact area of S with E .
ϑ_2	The contact area of E with S .
ρ	The disease transmission rate that is bi-linear.
d	The natural mortality rate.
b_1	The rate at which Q transforms into S .
b_2	The rate at which E turns into a quarantine.
w	The rate at which E transforms into I .
σ	The natural rate at which E transforms into R .
ξ	The natural rate at which I transforms into R .
c	The rate at which Q transforms into I .
β	The mortality rate for I .
u	The government policy parameter.
p	Some S becomes E due to media.

Lemma 2.3 (Ref. 43). If $0 < \alpha \leq 1$, $y(t) \in C[a, b]$, and ${}_a^C D_t^\alpha y(t) \in C(a, b]$, then

$$y(t) = y(a) + \frac{1}{(\alpha)} \left({}_a^C D_t^\alpha y \right) (\zeta) (t-a)^\alpha,$$

where $\zeta \in [a, t]$, $\forall t \in (a, b]$.

Corollary 2.1. Let $0 < \alpha \leq 1$, $y(t) \in C[a, b]$, and ${}_a^C D_t^\alpha y(t) \in C(a, b]$. Then $y(t)$ is non-increasing $\forall t \in [a, b]$, if ${}_a^C D_t^\alpha y(t) \leq 0$, $\forall t \in (a, b)$. While, $y(t)$ is non-decreasing $\forall t \in [a, b]$, if ${}_a^C D_t^\alpha y(t) \geq 0$, $\forall a < t < b$.

3. Model formulation

This section presents a fractional model for COVID-19. The total population is divided into five disease variables in the COVID-19 epidemic model, and the relationship between the variables is shown in Fig. 1, with the details of the variables is shown in Table 1.

Assume a model composed of five fractional differential equations as follows:

$$\begin{aligned} {}_0^C D_t^\alpha S &= A - \rho (1 - \vartheta_2) (1 - \vartheta_1) SE + b_1 Q - d S - p S u \\ {}_0^C D_t^\alpha E &= \rho (1 - \vartheta_2) (1 - \vartheta_1) SE - b_2 E - w E - \sigma E - d E \\ {}_0^C D_t^\alpha Q &= b_2 E - b_1 Q - c Q - d Q \\ {}_0^C D_t^\alpha I &= w E + c Q - (\xi + d + \beta) I \\ {}_0^C D_t^\alpha R &= \xi I + \sigma E - d R + p S u \end{aligned} \quad (3.1)$$

where $S(0) \geq 0$, $E(0) \geq 0$, $Q(0) \geq 0$, $I(0) \geq 0$ and $R(0) \geq 0$ are the initial conditions. Also, Table 2 shows the parameters in the COVID-19 fractional model (3.1).

Theorem 3.1 (Existence and Uniqueness). The COVID-19 fractional model (3.1) has unique solution for all $t \geq 0$.

Proof. For the model (3.1), let $y(t) = (S(t), E(t), Q(t), I(t), R(t))^T$ and $g(t, y(t)) = \begin{pmatrix} g_1(t, y(t)) \\ g_2(t, y(t)) \\ g_3(t, y(t)) \\ g_4(t, y(t)) \\ g_5(t, y(t)) \end{pmatrix} = \begin{pmatrix} A - \rho (1 - \vartheta_2) (1 - \vartheta_1) SE + b_1 Q - d S - p S u \\ \rho (1 - \vartheta_2) (1 - \vartheta_1) SE - b_2 E - w E - \sigma E - d E \\ b_2 E - b_1 Q - c Q - d Q \\ w E + c Q - (\xi + d + \beta) I \\ \xi I + \sigma E - d R + p S u \end{pmatrix}$.

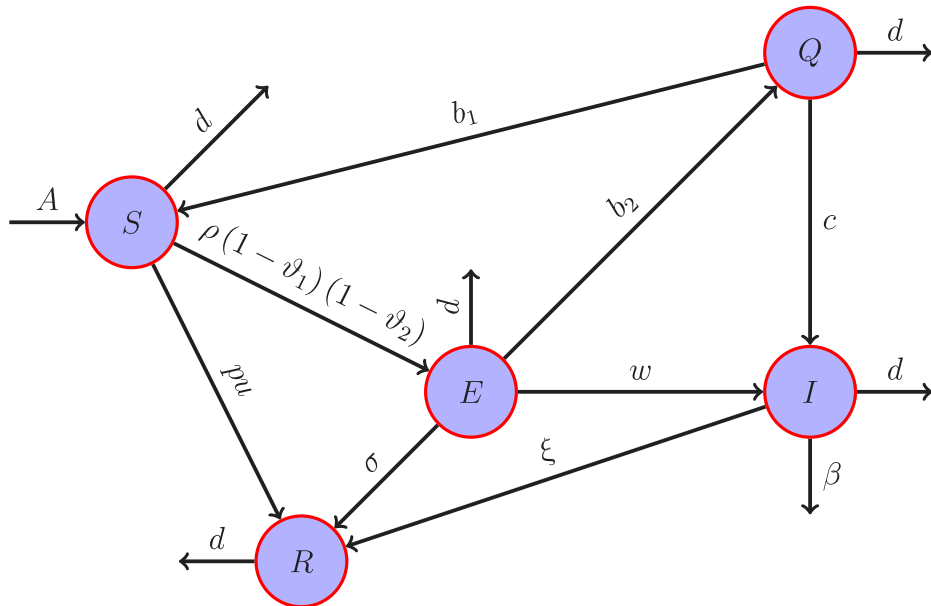


Fig. 1. COVID-19 infection model diagram.

It is clear that $g(t, y(t))$ is quadratic function so it is continuous with respect y on \mathbb{R}^5 , and Lebesgue-measurable for all $t \in \mathbb{R}$. Now, we compute $\|g(t, y(t))\|_1 = \sum_{j=1}^5 |g_j(t, y(t))|$

$$\begin{aligned} \|g(t, y(t))\|_1 &= |A - \rho(1 - \vartheta_2)(1 - \vartheta_1)SE + b_1Q - dS - pSu| \\ &\quad + |\rho(1 - \vartheta_2)(1 - \vartheta_1)SE - b_2E - wE - \sigma E - dE| \\ &\quad + |b_2E - b_1Q - cQ - dQ| + |\xi I + \sigma E - dR + pSu| \\ &\quad + |wE + cQ - (\xi + d + \beta)I| \end{aligned}$$

Applying the triangular inequality, one can have;

$$\begin{aligned} \|g(t, y(t))\|_1 &\leq A + 2\rho(1 - \vartheta_2)(1 - \vartheta_1)|S||E| + b_1|Q| + d|S| + 2pu|S| \\ &\quad + (2b_2 + 2w + 2\sigma + d)|E| + (b_1 + 2d + c)|Q| + d|R| \\ &\quad + (2\xi + d + \beta)|I| \end{aligned}$$

Since, $N = S + Q + E + I + R$ we have $S \leq N$. This imply

$$\begin{aligned} \|g(t, y(t))\|_1 &\leq A + (2\rho(1 - \vartheta_2)(1 - \vartheta_1)N + (2b_2 + 2w + 2\sigma + d))|E| \\ &\quad + (d + 2pu)|S| + (2b_1 + 2d + c)|Q| + d|R| + (2\xi + d + \beta)|I| \end{aligned}$$

Now, add the following positive terms to the RHS of the above inequality

$$\begin{aligned} &(2\rho(1 - \vartheta_2)(1 - \vartheta_1)N + 2b_2 + 2w + 2\sigma + 4d + 2b_1 + 2c + 2\xi + \beta)|S|, \\ &(2\rho(1 - \vartheta_2)(1 - \vartheta_1)N + 2b_2 + 2w + 2\sigma + 4d + 2pu + 2\xi + \beta)|Q|, \\ &(2\rho(1 - \vartheta_2)(1 - \vartheta_1)N + 2b_2 + 2w + 2\sigma + 4d + 2pu + 2b_1 + 2c)|I|, \\ &(2\rho(1 - \vartheta_2)(1 - \vartheta_1)N + 2b_2 + 2w + 2\sigma + 4d + 2pu + 2b_1 \\ &\quad + 2c + 2\xi + \beta)|R|, \\ &(4d + 2pu + 2b_1 + 2c + 2\xi + \beta)|E|, \end{aligned}$$

So, we have

$$\|g(t, y(t))\|_1 \leq \mu + \gamma \|y(t)\|, \quad \forall t \in \mathbb{R}, y(t) \in \mathbb{R}^5, \quad (3.2)$$

where the positive constants, $\mu = A$ and $\gamma = (2\rho(1 - \vartheta_2)(1 - \vartheta_1)N + (2b_2 + 2w + 2\sigma + d))(d + 2pu)(2b_1 + 2d + c)(2\xi + d + \beta)d$. By applying **Theorem 2.2**, we deduce that The COVID-19 fractional model (3.1) has a solution for all \mathbb{R} . Since, $g(t, y(t))$ is quadratic function so $\frac{\partial g(t, y(t))}{\partial y(t)}$ is continuous with respect y on \mathbb{R}^5 . By using **Lemma 2.2**, we deduce that The COVID-19 fractional model (3.1) has a unique solution for all \mathbb{R} .

Theorem 3.2. Consider $\bar{y}(t) = (\bar{S}(t), \bar{E}(t), \bar{Q}(t), \bar{I}(t), \bar{R}(t))^T$, then

$$\|(g(\xi, \bar{y}(\xi)) - g(\xi, y(\xi)))\|_1 \leq h\|\bar{y}(\xi) - y(\xi)\|_1$$

for some positive constant h .

The proof of **Theorem 3.2** is similar to proof **Theorem 3.1**, so we omitted it.

Now, if the initial values are non-negative, it is simple to show that the solutions of model (3.1) are always non-negative, as we will prove in **Theorem 3.3**.

Theorem 3.3. The admissible region $\Psi = \{(S, E, Q, I, R) \in \mathbb{R}^{+5} : S \geq 0, E \geq 0, Q \geq 0, I \geq 0, R \geq 0\}$ for model (3.1) is a positive invariant set.

Proof. The uniqueness and existence of the solution of model (3.1) has been proved in **Theorem 3.1**. Say the solution is $y(t) = (S(t), E(t), Q(t), I(t), R(t))^T$. Also, ${}^C D_t^\alpha y$ continuous function, since $g(t, y(t))$ is quadratic function. However, let us try to compute ${}^C D_t^\alpha S|_{S=0}$, ${}^C D_t^\alpha E|_{E=0}$, ${}^C D_t^\alpha Q|_{Q=0}$, ${}^C D_t^\alpha I|_{I=0}$, and ${}^C D_t^\alpha R|_{R=0}$ by substitute $S = 0$ in the first equation of model (3.1), $E = 0$ in the second equation of model (3.1), $Q = 0$ in the third equation of model (3.1), $I = 0$ in the fourth equation of model (3.1), and $R = 0$ in the fifth equation of model (3.1). Since all parameter in model (3.1) is positive constants, we have

$$\begin{aligned} {}^C D_t^\alpha S|_{S=0} &= A + b_1Q \geq 0 \\ {}^C D_t^\alpha E|_{E=0} &= 0 \\ {}^C D_t^\alpha Q|_{Q=0} &= b_2E \geq 0 \\ {}^C D_t^\alpha I|_{I=0} &= wE + cQ \geq 0 \\ {}^C D_t^\alpha R|_{R=0} &= \xi I + \sigma E + pSu \geq 0 \end{aligned} \quad (3.3)$$

for all $t \geq 0$. Now, from the second equation in Eq. (3.3), Now, let initial condition of model (3.1) lie in Ψ . According to Eq. (3.3) and Corollary 2.1 we find that $(S(t), E(t), Q(t), I(t), R(t)) \in \Psi$. This result means that Ψ is a positive invariant set of solution for model (3.1).

Theorem 3.4. For the COVID-19 fractional model (3.1), the admissible region Ψ is uniformly bounded.

Proof. From (3.1) the total population satisfies

$${}^C D_t^\alpha N(t) = A - dN(t) - \varepsilon I(t).$$

where

$$N(t) = S(t) + E(t) + Q(t) + I(t) + R(t).$$

$${}_0^C D_t^\alpha N(t) \leq A - dN(t)$$

Now by using the Laplace transform for Eq. (3.3) we can get the following equation

$$\begin{aligned} s^\alpha L\{N(t)\} - s^{\alpha-1}N(0) &\leq \frac{A}{s} - dL\{N(t)\} \\ (s^\alpha + d)L\{N(t)\} &\leq \frac{A}{s} + s^{\alpha-1}N(0) \\ L\{N(t)\} &\leq \frac{s^{-1}}{s^\alpha + d}A + \frac{s^{\alpha-1}}{s^\alpha + d}N(0) \\ \text{Then from Eq. (5) and Eq. (6) we get} \\ N(t) &\leq At^\alpha E_{\alpha,\alpha+1}(-dt^\alpha) + E_{\alpha,1}(-dt^\alpha)N(0) \\ &\leq \frac{A}{d}[dt^\alpha E_{\alpha,\alpha+1}(-dt^\alpha) + E_{\alpha,1}(-dt^\alpha)] \\ &\leq \frac{A}{d}\left[dt^\alpha E_{\alpha,\alpha+1}(-dt^\alpha) - dt^\alpha E_{\alpha,\alpha+1}(-dt^\alpha) + \frac{1}{(1)}\right] \\ &\leq \frac{A}{d} \end{aligned} \quad (3.4)$$

Solutions in the model (3.1) are restricted as follows

$$\Psi = \{(S, E, Q, I, R) \in R^{+5} : 0 \leq N(t) \leq \frac{A}{d}\}$$

3.1. Infection equilibria points

There are two equilibria in the Caputo fractional model (3.1). The disease-free equilibria Ξ_0 , in which infection is eradicated from the body is given as follows:

$$\Xi_0 = (S_0, E_0, Q_0, I_0, R_0) = \left(\frac{A}{d+pu}, 0, 0, 0, \frac{puA}{d(d+pu)} \right).$$

If $A\rho(1-\vartheta_1)(1-\vartheta_2) \geq (d+pu)(b_2+w+\sigma+d)$, then there is other type of equilibrium which is called endemic equilibria Ξ^* = $(S^*, E^*, Q^*, I^*, R^*)$, which occurs when the infection is always present in the model, where

$$S^* = \frac{b_2+w+\sigma+d}{(1-\vartheta_1)(1-\vartheta_2)\rho},$$

$$E^* = \frac{A\rho(1-\vartheta_1)(1-\vartheta_2)(b_1+d+c) - (d+pu)(b_2+w+\sigma+d)(b_1+d+c)}{(1-\vartheta_1)(1-\vartheta_2)\rho[b_2(d+c)+(w+\sigma+d)(b_1+d+c)]},$$

$$Q^* = \frac{b_2A\rho(1-\vartheta_1)(1-\vartheta_2) - b_2(d+pu)(b_2+w+\sigma+d)}{(1-\vartheta_1)(1-\vartheta_2)\rho[b_2(d+c)+(w+\sigma+d)(b_1+d+c)]},$$

$$I^* = \frac{[w(b_1+d+c)+b_2c][A\rho(1-\vartheta_1)(1-\vartheta_2) - (d+pu)(b_2+w+\sigma+d)]}{(1-\vartheta_1)(1-\vartheta_2)\rho[\xi+d+\beta[b_2(d+c)+(w+\sigma+d)(b_1+d+c)]]},$$

$$R^* = \frac{puS^* + \sigma E^* + \xi I^*}{d}.$$

3.2. Calculating R_0 .

The BRN, R_0 , is the most important epidemiological component for classifying the type of infection. In fact, R_0 is defined as the total secondary number of people infected as a result of one infected person over the course of the entire time interval. Consequently, R_0 is a non-dimensional quantity that measures the probability of a disease spreading. However, R_0 is defined as the “number of secondarily infected individuals caused by a single infected individual over the entire time interval”.⁴⁴ As a result, R_0 is a dimensionless quantity that denotes the likelihood of the disease spreading. There are several techniques available for determining R_0 for epidemic spread. The next-generation

matrix approach^{45,46} is used in our current research article. Only E , Q and I are currently directly involved in the spread of disease. As a result of system (3.1), we have

$$\begin{aligned} {}_0^C D_t^\alpha E &= \rho(1-\vartheta_1)(1-\vartheta_2)SE - b_2E - wE - \sigma E - dE \\ {}_0^C D_t^\alpha Q &= b_2E - b_1Q - cQ - dQ \\ {}_0^C D_t^\alpha I &= wE + cQ - (\eta+d+\beta)I \end{aligned} \quad (3.5)$$

According in the procedure in Ref. 44, we rewrite the system (3.5) as ${}_0^C D_t^\alpha x = P(x) - \Theta(x)$, where

$$x = \begin{bmatrix} E \\ Q \\ I \end{bmatrix}, P(x) = \begin{bmatrix} \rho(1-\vartheta_1)(1-\vartheta_2)SE \\ 0 \\ 0 \end{bmatrix}, \text{ and} \\ \Theta(x) = \begin{bmatrix} (b_2+w+\sigma+d)E \\ (b_1+c+d)Q - b_2E \\ (\eta+d+\beta)I - wE - cQ \end{bmatrix}$$

We note from the system (3.5) that $E_0 = \left(\frac{A}{d+pu}, 0, 0, 0, \frac{puA}{d(d+pu)}\right)$ is a disease-free equilibrium. The Jacobean matrix of $\rho(x)$ at point E_0 , is given by:

$$N = \mathfrak{J}(P|E_0) = \begin{pmatrix} \rho(1-\vartheta_1)(1-\vartheta_2) \frac{A}{d+pu} & 0 & 0 \\ 0 & 0 & 0 \\ 0 & 0 & 0 \end{pmatrix} \quad (3.6)$$

Also, the Jacobean matrix of Θ at point E_0 , is given by:

$$M = \mathfrak{J}(\Theta|E_0) = \begin{pmatrix} b_2+w+\sigma+d & 0 & 0 \\ -b_2 & b_1+c+d & 0 \\ -w & -c & \eta+d+\beta \end{pmatrix} \quad (3.7)$$

The inverse of M is given by;

$$M^{-1} = \begin{pmatrix} \frac{1}{b_2+w+\sigma+d} & 0 & 0 \\ \frac{b_2}{(b_2+w+\sigma+d)(b_1+c+d)} & \frac{1}{b_1+c+d} & 0 \\ \frac{w(b_1+c+d)+b_2c}{(b_2+w+\sigma+d)(b_1+c+d)(\eta+d+\beta)} & \frac{c}{(b_1+c+d)(\eta+d+\beta)} & \frac{1}{\eta+d+\beta} \end{pmatrix} \quad (3.8)$$

The next generation matrix NM^{-1} is given by;

$$G = NM^{-1} = \begin{pmatrix} \frac{A\rho(1-\vartheta_1)(1-\vartheta_2)}{(d+pu)(b_2+w+\sigma+d)} & 0 & 0 \\ 0 & 0 & 0 \\ 0 & 0 & 0 \end{pmatrix} \quad (3.9)$$

The eigenvalues from the matrix G are $\lambda_1 = 0$, $\lambda_2 = 0$, and $\lambda_3 = \frac{A\rho(1-\vartheta_1)(1-\vartheta_2)}{(d+pu)(b_2+w+\sigma+d)}$. As a result, the reproductive number R_0 (which is the largest eigenvalue) is calculated as follows:

$$R_0 = \frac{A\rho(1-\vartheta_1)(1-\vartheta_2)}{(d+pu)(b_2+w+\sigma+d)} \quad (3.10)$$

3.3. Sensitivity analysis

Due to the fact that R_0 is an extremely biologically significant quantity that plays a chief role in the spread of any pandemic, investigating the sensitivity of R_0 is very interesting and crucial to the elimination and effective control of the disease. R_0 sensitivity to changes in parameter Y is represented by this index. So, we can calculate the changes in all parameters in the formula of R_0 by using the partial derivatives as follows:

Now, we give the following relationship that describes the R_0 forward sensitivity index with respect to the parameter Y :

$$\Xi_Y^{R_0} = \left(\frac{\partial R_0}{\partial Y} \right) \left(\frac{Y}{R_0} \right) \quad (3.11)$$

where Y is a parameter to describe the basic reproductive number R_0 . It is well known that a negative (positive) index means that any increase in the parameter Y leads to a decrease (increase) in R_0 .⁴⁷ The sensitivity indices with respect to the parameters can be given A , ϑ_1 , ϑ_2 ,

$$\mathfrak{J} = \begin{pmatrix} -(d + pu) & -\rho(1 - \vartheta_1)(1 - \vartheta_2) \frac{A}{d + pu} & b_1 & 0 & 0 \\ 0 & \rho(1 - \vartheta_1)(1 - \vartheta_2) S_0 - (b_2 + w + \sigma + d) & 0 & 0 & 0 \\ 0 & b_2 & -(b_1 + d + c) & 0 & 0 \\ 0 & w & c & -(\xi + d + \beta) & 0 \\ pu & \sigma & 0 & \xi & -d \end{pmatrix}$$

Box I.

Table 3
Sensitivity indices.

Parameters	The sensitivity index of R_0 with respect to the parameters	Indexes of sensitivity
A	1	+ve
ρ	1	+ve
ϑ_1	$\frac{-\vartheta_1}{1-\vartheta_1}$	-ve
ϑ_2	$\frac{-\vartheta_2}{1-\vartheta_2}$	-ve
d	$\frac{-d(pu+2d+\sigma+w+b_2)}{(b_2+w+\sigma+d)(pu+d)}$	-ve
p	$\frac{-up}{pu+d}$	-ve
b_2	$\frac{-b_2}{b_2+w+\sigma+d}$	-ve
w	$\frac{-w}{b_2+w+\sigma+d}$	-ve
u	$\frac{-up}{pu+d}$	-ve
σ	$\frac{-\sigma}{b_2+w+\sigma+d}$	-ve

ρ , d , b_1 , w , u , p , and σ respectively, by the basic reproductive number mentioned in the Eq. (3.10), as in Table 3.

3.4. Stability analysis of COVID-19 model

In this section, we look for stability that is local to the equilibrium Ξ_0 and the equilibrium Ξ^* .

Theorem 3.5. *The model (3.1) is locally asymptotic stable when $R_0 < 1$ at Ξ_0 and unstable when $R_0 > 1$.*

Proof. The Jacobian matrix of the model (3.1) at the equilibrium Ξ_0 is given as follows: see \mathfrak{J} that is given in Box I. The eigenvalue equation of the \mathfrak{J} at the equilibrium Ξ_0 is

$$(\lambda + d)(\lambda + \xi + d + \beta)(\lambda + b_1 + d + c)(\lambda + d + pu) \times (\lambda + (b_2 + w + \sigma + d)(1 - R_0)) = 0$$

$$\begin{aligned} \lambda_1 &= -d \\ \lambda_2 &= -\xi - d - \beta \\ \lambda_3 &= -b_1 - c - d \\ \lambda_4 &= -up - d \\ \lambda_5 &= -(b_2 + w + \sigma + d)(1 - R_0) \end{aligned}$$

We can note $\lambda_1, \lambda_2, \lambda_3, \lambda_4$ have a real negative part and $\lambda_5 < 0$ has a real negative part when $R_0 < 1$. As a result, the model (3.1) is locally asymptotically stable when $R_0 < 1$, whereas it is unstable when $R_0 > 1$ and so the theorem was proven.

Theorem 3.6. *If the endemic equilibrium, Ξ^* , exists, then it is locally asymptotically stable.*

Proof. From the model (3.1) the Jacobean matrix at equilibrium Ξ^* we can get as follows: see \mathfrak{J} that is given in Box II.

The eigenvalue polynomial of the model (3.1) at the equilibrium Ξ^* , is given as follows:

$$(\lambda + d)(\lambda + \xi + d + \beta)(\lambda^3 + A_1\lambda^2 + A_2\lambda + A_3) = 0 \quad (3.12)$$

where $A_1 = (1 - \vartheta_1)(1 - \vartheta_2)\rho + 2d + b_1 + c + pu$, $A_2 = (d + pu + \rho(1 - \vartheta_1)(1 - \vartheta_2)E^*)(b_1 + d + c) + (b_2 + w + \sigma + d)\rho(1 - \vartheta_1)(1 - \vartheta_2)$, and $A_3 = \rho(1 - \vartheta_1)(1 - \vartheta_2)E^*[b_2 + w + \sigma + d](b_1 + d + c) - b_1 b_2]$

Indeed, one can notice that Eq. (3.12) have two negative roots and the other roots are the roots of the cubic equation $\lambda^3 + A_1\lambda^2 + A_2\lambda + A_3 = 0$. If these roots lie inside the complex plane which satisfies $|\arg(\lambda)| > \frac{\alpha\pi}{2}$ and by using Theorem 2.1, We can conclude that the model (3.1) is asymptotically stable locally close to its endemic equilibrium Ξ^* because A_1, A_2, A_3 , and $A_1 A_2 - A_3$ are always positive regardless of the parametric value.

3.5. Hyers–Ulam stability

To study the global stability of the considered fractional model (3.1), we use the Ulam–Hyers sense. For this purpose, we define the following inequality:

$$\left| {}_0^C D_t^\alpha y(t) - g(t, y(t)) \right| \leq \varepsilon, \quad \forall t \in [0, T]. \quad (3.13)$$

Now, $\bar{y} \in \Sigma$ is solution of (10) if and only if there is $h \in \Sigma$ such that:

i | $h(t)$ | $\leq \varepsilon$.

ii

$${}_0^C D_t^\alpha \bar{y}(t) = g(t, \bar{y}(t)) + h(t), \quad \forall t \in [0, T]. \quad (3.14)$$

Now, apply the fractional R-LF integral to both sides of (3.14), one can have

$$\begin{aligned} \bar{y}(t) &= \bar{y}(0) + \frac{1}{\Gamma(\alpha)} \int_0^t (t - \xi)^{\alpha-1} g(\xi, \bar{y}(\xi)) d\xi \\ &\quad + \frac{1}{\Gamma(\alpha)} \int_0^t (t - \xi)^{\alpha-1} h(\xi) d\xi, \quad \forall t \in [0, T]. \end{aligned}$$

By taken condition (i), we get

$$\begin{aligned} |\bar{y}(t) - \bar{y}(0) - \frac{1}{\Gamma(\alpha)} \int_0^t (t - \xi)^{\alpha-1} g(\xi, \bar{y}(\xi)) d\xi| \\ \leq \frac{\varepsilon}{\Gamma(\alpha)} \int_0^t (t - \xi)^{\alpha-1} d\xi, \quad \forall t \in [0, T]. \end{aligned}$$

So, we have

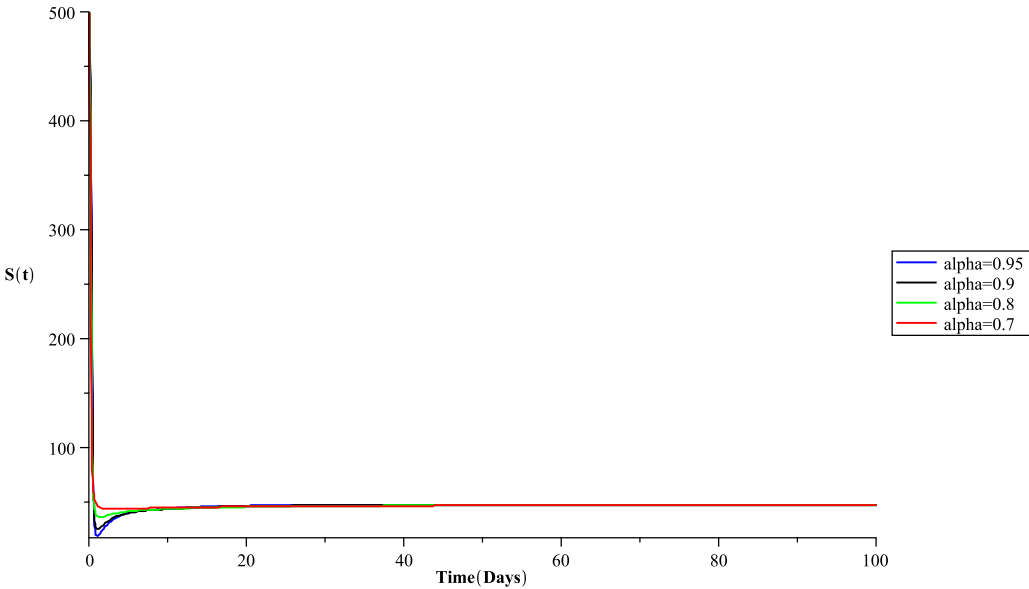
$$|\bar{y}(t) - \bar{y}(0) - \frac{1}{\Gamma(\alpha)} \int_0^t (t - \xi)^{\alpha-1} g(\xi, \bar{y}(\xi)) d\xi| \leq \frac{\varepsilon T^\alpha}{\Gamma(\alpha + 1)}, \quad \forall t \in [0, T]. \quad (3.15)$$

Definition 3.1. The COVID-19 fractional model (3.1) is Hyers–Ulam stability on $[0, T]$ if there exists a constant $Y_g > 0$ such that for any $\varepsilon > 0$, and any $\bar{y}(t)$ satisfying (3.13), then the COVID-19 fractional model (3.1) possess a solution $y(t)$ satisfying

$$\|\bar{y}(t) - y(t)\|_1 \leq \varepsilon Y_g, \quad \forall t \in [0, T].$$

$$\mathfrak{J} = \begin{pmatrix} -\rho(1-\vartheta_1)(1-\vartheta_2)E^* - (d+pu) & -\rho(1-\vartheta_1)(1-\vartheta_2)S^* & b_1 & 0 & 0 \\ \rho(1-\vartheta_1)(1-\vartheta_2)E^* & \rho(1-\vartheta_1)(1-\vartheta_2)S^* - (b_2+w+\sigma+d) & 0 & 0 & 0 \\ 0 & b_2 & -(b_1+d+c) & 0 & 0 \\ 0 & w & c & -(\xi+d+\beta) & 0 \\ pu & \sigma & 0 & \xi & -d \end{pmatrix}$$

Box II.

Fig. 2. The susceptible population, $S(t)$, for various value of α .

Theorem 3.7. Assume the assumptions (i) and (ii) holds. Then the COVID-19 fractional model (3.1) is Hyers–Ulam stability on $[0, T]$, if $\Gamma(\alpha + 1) > T^\alpha h$ hold.

Proof. Recall Theorem 3.1, we let $y(t)$ be a unique solution of the COVID-19 fractional model (3.1), let $\bar{y}(t)$ satisfy (3.13). By applying the fractional R-LF integral to both sides of (3.1), we get

$$y(t) = y(0) + \frac{1}{\Gamma(\alpha)} \int_0^t (t-\xi)^{\alpha-1} g(\xi, y(\xi)) d\xi, \forall t \in [0, T]. \quad (3.16)$$

Now, using (3.15) and (3.16), we compute $\|\bar{y}(t) - y(t)\|_1$ as follows:

$$\|\bar{y}(t) - y(t)\|_1 = \left\| \bar{y}(t) - y(0) - \frac{1}{\Gamma(\alpha)} \int_0^t (t-\xi)^{\alpha-1} g(\xi, y(\xi)) d\xi \right\|_1$$

By adding and subtracting the term $\frac{1}{\Gamma(\alpha)} \int_0^t (t-\xi)^{\alpha-1} g(\xi, \bar{y}(\xi)) d\xi$ and applying the triangle inequality, we have

$$\begin{aligned} \|\bar{y}(t) - y(t)\|_1 &\leq \left\| \bar{y}(t) - y(0) - \frac{1}{\Gamma(\alpha)} \int_0^t (t-\xi)^{\alpha-1} g(\xi, \bar{y}(\xi)) d\xi \right\|_1 \\ &\quad + \left\| \frac{1}{\Gamma(\alpha)} \int_0^t (t-\xi)^{\alpha-1} (g(\xi, \bar{y}(\xi)) - g(\xi, y(\xi))) d\xi \right\|_1. \end{aligned}$$

Using (3.15) and the norm properties, one can get

$$\|\bar{y}(t) - y(t)\|_1 \leq \frac{\varepsilon T^\alpha}{\Gamma(\alpha+1)} + \frac{1}{\Gamma(\alpha)} \int_0^t (t-\xi)^{\alpha-1} \|g(\xi, \bar{y}(\xi)) - g(\xi, y(\xi))\|_1 d\xi$$

Applying Theorem 3.2, yields

$$\|\bar{y}(t) - y(t)\|_1 \leq \frac{\varepsilon T^\alpha}{\Gamma(\alpha+1)} + \frac{T^\alpha h}{\Gamma(\alpha+1)} \|\bar{y}(t) - y(t)\|_1.$$

So, we have $\|\bar{y}(t) - y(t)\|_1 \leq Y_g \varepsilon$, where $Y_g = \frac{T^\alpha}{\Gamma(\alpha+1)-T^\alpha h}$. Using Definition 3.1, we deduce that the COVID-19 fractional model (3.1) is Hyers–Ulam stability on $[0, T]$.

4. Numerical simulations

It is common knowledge that there is no analytical method currently available to solve FDEs. Consequently, to find approximations of solutions to FDEs, accurate and efficient numerical methods are needed, such as the generalized fractional differential transform,⁴⁸ the fractional difference method,⁴⁹ the power series method,⁵⁰ the fractional variational iteration method,⁵¹ the Haar wavelet collocation,⁵² the restricted fractional differential transform,⁵³ the wavelet method,⁵⁴ the fractional Adams method,⁵⁵ the spectral method,⁵⁶ and also numerous additional outstanding works in the following papers (see e.g. Refs. 57–64). However, to give a complete picture of the stability analysis in the previous section, we will use the fractional Euler method (FEM)³⁷ to solve the model numerically. To underpin the analysis in this work, we will investigate the effect of fractional order on stability behavior by taking $\alpha = 0.95, 0.9, 0.8, 0.7$.

In order to use the FEM for solving the fractional model (3.1), we rewrite the interval $[0, T]$ into n subintervals $[(k-1)h, kh]$, $\forall k = 1, 2, \dots, n$ with $h = \frac{T}{n}$. As a result, we have the discretized equations shown below:

$$\begin{aligned} S(t_k) &= S(0) + \frac{h^\alpha}{\Gamma(\alpha+1)} \sum_{i=0}^k \chi_{k,i} [\Lambda - \rho(1-\vartheta_2)(1-\vartheta_1) S(t_i) E(t_i) \\ &\quad + b_1 Q(t_i) - d S(t_i) - p S(t_i) u] \\ E(t_k) &= E(0) + \frac{h^\alpha}{\Gamma(\alpha+1)} \sum_{i=0}^k \chi_{k,i} [\rho(1-\vartheta_2)(1-\vartheta_1) S(t_i) E(t_i) \\ &\quad - b_2 E(t_i) - w E(t_i) - \sigma E(t_i) - d E(t_i)] \\ Q(t_k) &= Q(0) + \frac{h^\alpha}{\Gamma(\alpha+1)} \sum_{i=0}^k \chi_{k,i} [b_2 E(t_i) - b_1 Q(t_i) - c Q(t_i) - d Q(t_i)] \end{aligned}$$

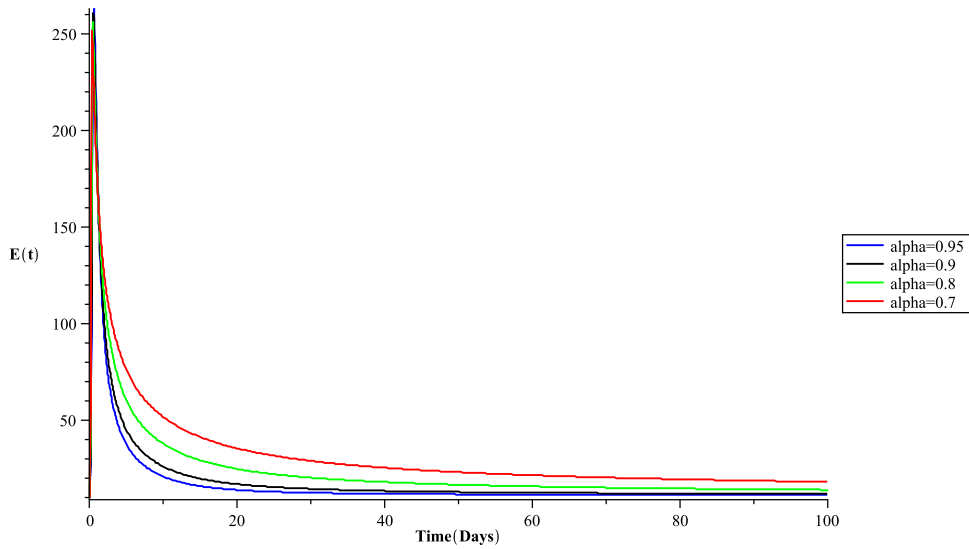


Fig. 3. The exposed population, $E(t)$, for various value of α .

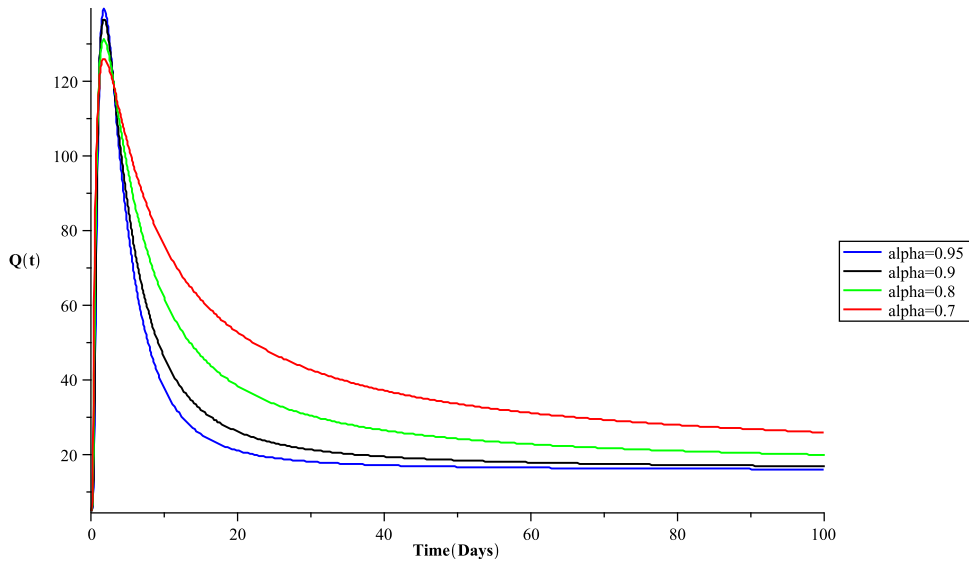


Fig. 4. The population that is quarantined, $Q(t)$, for various value of α .

$$\begin{aligned} I(t_k) &= I(0) + \frac{h^\alpha}{\Gamma(\alpha+1)} \sum_{i=0}^k \chi_{k,i} [wE(t_i) + cQ(t_i) - (\xi + d + \beta) I(t_i)] \\ R(t_k) &= R(0) + \frac{h^\alpha}{\Gamma(\alpha+1)} \sum_{i=0}^k \chi_{k,i} [\xi I(t_i) + \sigma E(t_i) - dR(t_i) + pS(t_i)u] \end{aligned}$$

where $\chi_{k,i} = (k-i)^\alpha - (k-1-i)^\alpha$, $\forall i = 0, 1, \dots, k$, and $\forall k = 1, 2, \dots, n$.

Using FEM, precise numerical solutions can be obtained over an extended period of time. As a starting point, we used the following initial conditions: $(S(0), E(0), Q(0), I(0), R(0)) = (500, 10, 5, 0, 0)$ with the following cases.

Case 1: In this case, we use the following values of parameters; $A = 50$, $d = 0.2$, $b_1 = 0.25$, $b_2 = 0.8$, $c = 0.12$, $\rho = 1.5$, $\sigma = 0.2$, $\vartheta_1 = 0.78$, $\vartheta_2 = 0.92$, $w = 0.0714$, $p = 5$, $\xi = 0.025$, $u = 0.8$ and $\beta = 0.25$.⁶⁵

Now, recall Eq. (28) and compute reproductive number, we find $R_0 = 1.259982498$. So, the endemic equilibria $\Xi^* = (48.15909091, 11.20766266, 15.73005285, 5.658596752, 162.1713509)$ is locally asymptotically stable according [Theorem 3.6](#) for various value of α . In fact, this is clearly through [Figs. 2–6](#).

Case 2: In this case, we use the following values of parameters; $A = 50$, $d = 0.2$, $b_1 = 0.25$, $b_2 = 0.8$, $c = 0.12$, $\rho = 1.5$, $\sigma = 0.2$, $\vartheta_1 = 0.78$, $\vartheta_2 = 0.92$, $w = 0.0714$, $p = 5$, $\xi = 0.025$, $u = 0.8$ and $\beta = 0.25$.⁶⁵

Now, recall Eq. (28) and compute reproductive number, we find $R_0 = 0.2471965662$. So, the disease-free equilibria $\Xi_0 = (60.67961165, 0, 0, 0, 189.3203883)$ is locally asymptotically stable according [Theorem 3.5](#). In fact, this is clearly through [Figs. 7–11](#).

5. Conclusions

This study focused on the investigation of a five-dimensional fractional-order COVID-19 mathematical model. We proved some theorems related to the existence, uniqueness, and positively invariant of this model's solution. Also, the basic reproductive number, R_0 , has been calculated in detail by using the next-generation matrix technique. Then the local asymptotic stability of the disease-free and endemic equilibriums have been studied. Additionally, we investigate the global stability of the proposed model in terms of the Ulam–Hyers criteria. Finally, we demonstrated the validity of our analysis by presenting

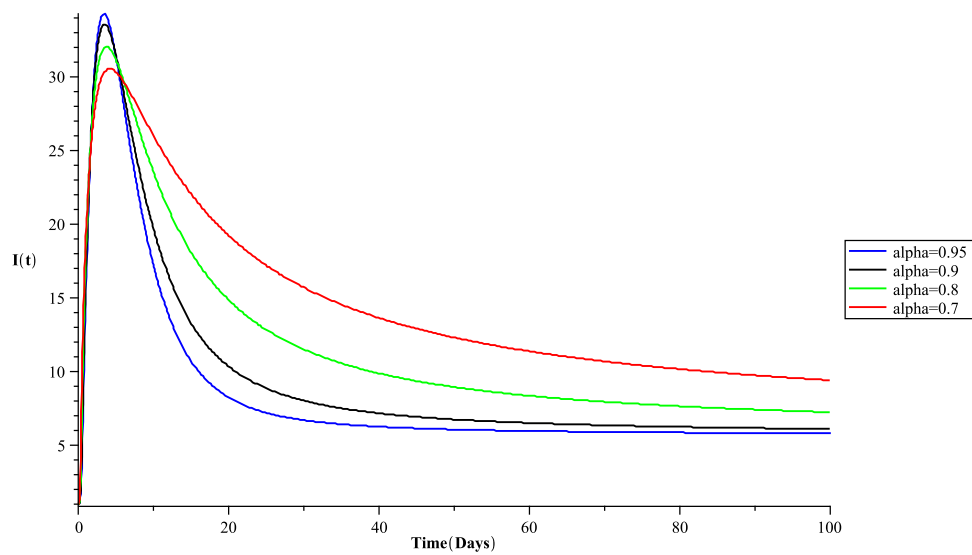


Fig. 5. The hospitalized infected population, $I(t)$, for various value of α .

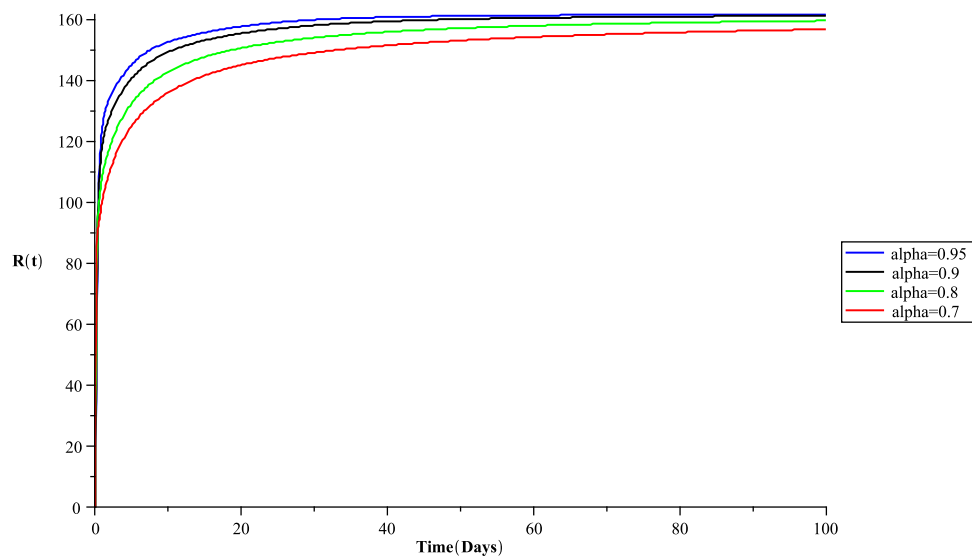


Fig. 6. The recovered or Removed population, $R(t)$, for various value of α .

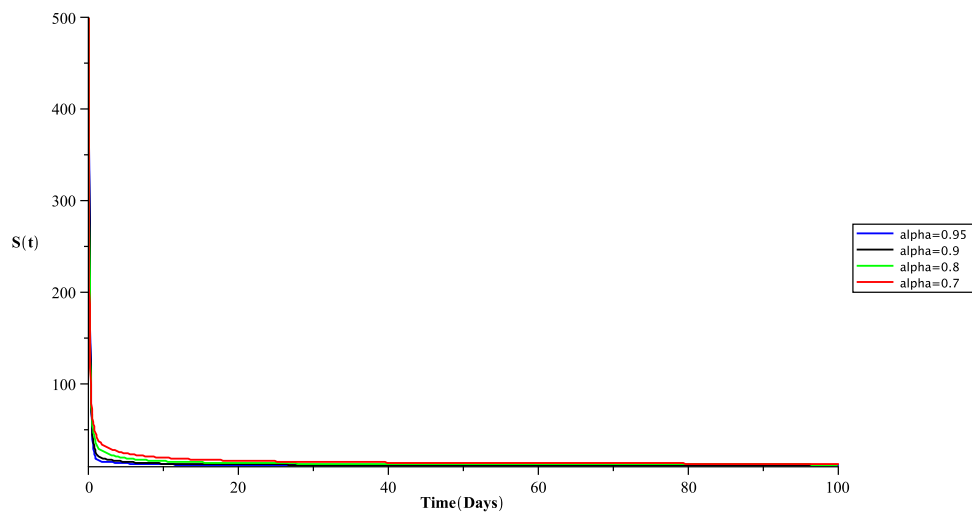


Fig. 7. The susceptible population, $S(t)$, for various value of α .

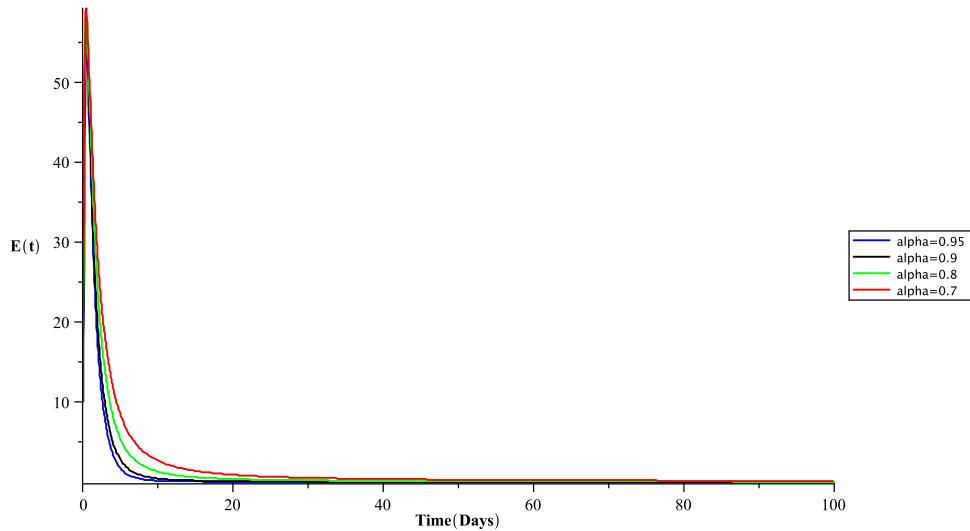


Fig. 8. The exposed population, $E(t)$, for various value of α .

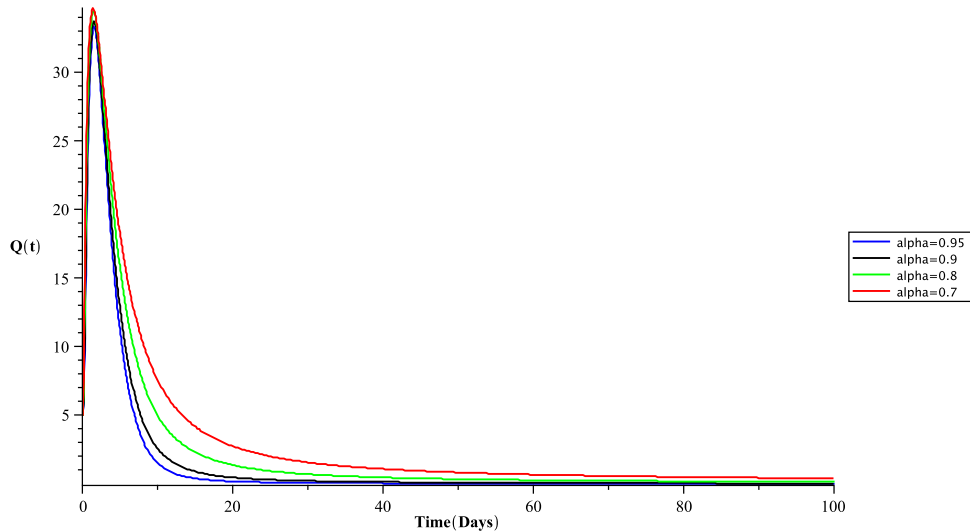


Fig. 9. The population that is quarantined, $Q(t)$, for various value of α .

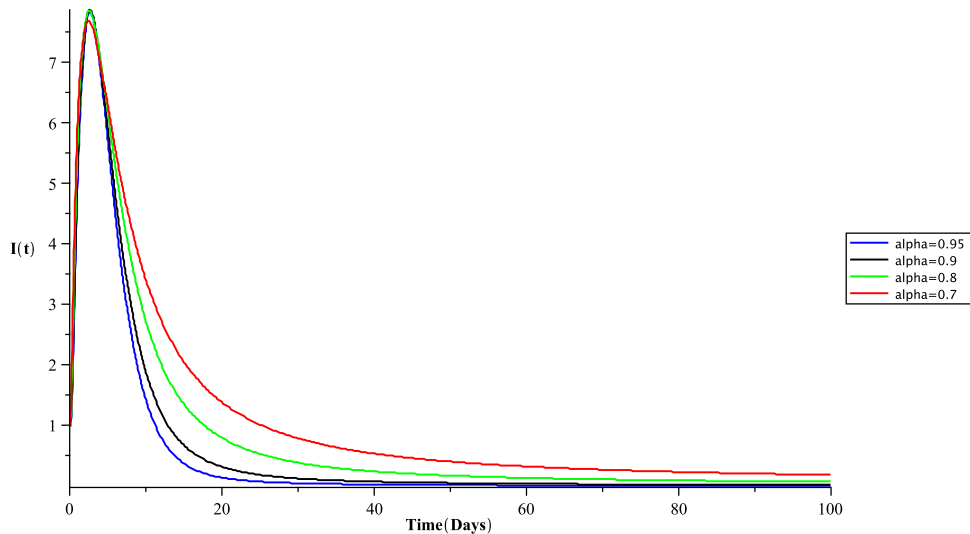


Fig. 10. The hospitalized infected population, $I(t)$, for various value of α .

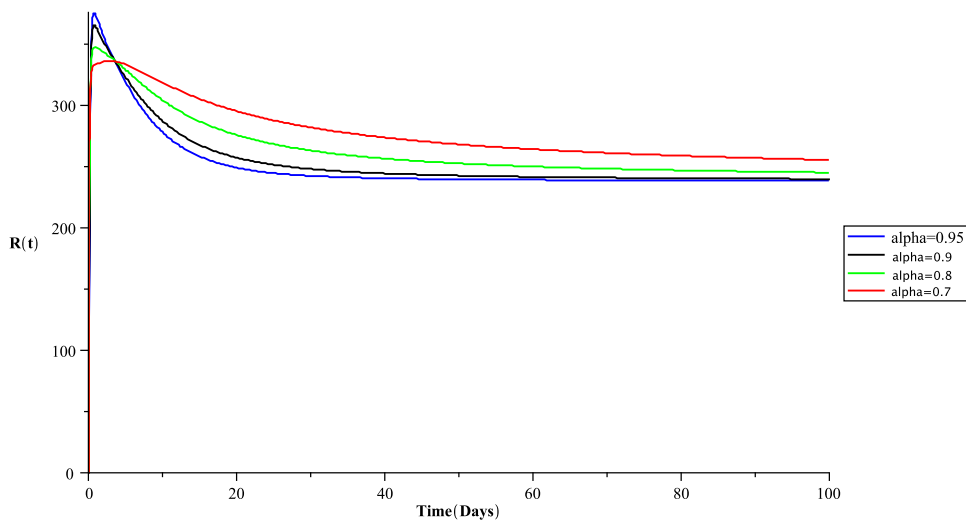


Fig. 11. The recovered or Removed population, $R(t)$, for various value of α .

an explanatory numerical simulation of the behavior of this model for various fractional order values.

Declaration of competing interest

The authors declare that they have no known competing financial interests or personal relationships that could have appeared to influence the work reported in this paper.

Data availability

No data was used for the research described in the article.

References

1. Guan Wei-jie, Ni Zheng-yi, Hu Yu, hua Liang Wen, Ou Chun-quan, He Jian-xing, Liu Lei, Shan Hong, Lei Chun-liang, Hui David SC, Du Bin, Li Lan-juan, Zeng Guang, Yuen Kwok-Yung, chong Chen Ru, Tang Chun-li, Wang Tao, yan Chen Ping, Xiang Jie, Li Shi-yue, Wang Jin-lin, Liang Zi-jing, Peng Yi-xiang, Wei Li, Liu Yong, Hu Ya-hua, Peng Peng, Wang Jian-ming, Liu Ji-yang, Chen Zhong, Li Gang, Zheng Zhi-jian, Qiu Shao-qin, Luo Jie, Ye Chang-jiang, Zhu Shao-yong, Zhong Nan-shan. Clinical characteristics of coronavirus disease 2019 in China. *N Engl J Med.* 2020;382(18):1708–1720.
2. Zarin Rahat. Numerical study of a nonlinear COVID-19 pandemic model by finite difference and meshless methods. *Partial Differ Equ Appl Math.* 2022;6:100460.
3. Ssebuliba J, Nakakawa JN, Ssematimba A, Mugisha JYT. Mathematical modelling of COVID-19 transmission dynamics in a partially comorbid community. *Partial Differ Equ Appl Math.* 2022;5:100212.
4. Velavan Thirumalaisamy P, Meyer Christian G. The COVID-19 epidemic. *Trop Med In Health.* 2020;25(3):278–280.
5. Wu Zunyou, McGoogan Jennifer M. Characteristics of and important lessons from the coronavirus disease 2019 (COVID-19) outbreak in China. *JAMA.* 2020;323(13):1239.
6. Roddam Andrew W. Mathematical epidemiology of infectious diseases: Model building, analysis and interpretation. *Int J Epidemiol.* 2001;30(1):186.
7. Hethcote Herbert W. The mathematics of infectious diseases. *SIAM Rev.* 2000;42(4):599–653.
8. Lazima ZA, Khalaf SL. Optimal control design of the in-vivo HIV fractional model. *Iraqi J Sci.* 2022;63(9):3877–3888.
9. Lin Qianying, Zhao Shi, Gao Daozhou, Lou Yijun, Yang Shu, Musa Salihu S, Wang Maggie H, Cai Yongli, Wang Weiming, Yang Lin, He Daihai. A conceptual model for the coronavirus disease 2019 (COVID-19) outbreak in Wuhan, China with individual reaction and governmental action. *Int J Infect Dis.* 2020;93:211–216.
10. Anastassopoulou Cleo, Russo Lucia, Tsakris Athanasios, Siettos Constantinos. Data-based analysis, modelling and forecasting of the COVID-19 outbreak. In: Othumpangat Sreekumar, ed. *PLOS ONE.* 2020;15(3):e0230405.
11. Asamoah Joshua Kiddy K, Owusu Mark A, Jin Zhen, Oduro FT, Abidemi Afeez, Gyasi Esther Opoku. Global stability and cost-effectiveness analysis of COVID-19 considering the impact of the environment: using data from Ghana. *Chaos Solitons Fractals.* 2020;140:110103.
12. Asamoah Joshua Kiddy K, Bornaa CS, Seidu Baba, Jin Zhen. Mathematical analysis of the effects of controls on transmission dynamics of SARS-CoV-2. *Alex Eng J.* 2020;59(6):5069–5078.
13. Casella Francesco. Can the COVID-19 epidemic be controlled on the basis of daily test reports? *IEEE Control Syst Lett.* 2021;5(3):1079–1084.
14. Asamoah Joshua Kiddy K, Jin Zhen, Sun Gui-Quan, Seidu Baba, Yankson Ernest, Abidemi Afeez, Oduro FT, Moore Stephen E, Okyere Eric. Sensitivity assessment and optimal economic evaluation of a new COVID-19 compartmental epidemic model with control interventions. *Chaos Solitons Fractals.* 2021;146:110885.
15. Faniran Taye Samuel, Ali Aatif, Al-Hazmi Nawal E, Asamoah Joshua Kiddy K, Nofal Taher A, Adewole Matthew O. New variant of SARS-CoV-2 dynamics with imperfect vaccine. In: Selişteanu Dan, ed. *Complexity.* 2022;2022:1–17.
16. Asamoah Joshua Kiddy K, Okyere Eric, Abidemi Afeez, Moore Stephen E, Sun Gui-Quan, Jin Zhen, Acheampong Edward, Gordon Joseph Frank. Optimal control and comprehensive cost-effectiveness analysis for COVID-19. *Results Phys.* 2022;33:105177.
17. Moore Stephen E, Nyandjo-Bamen Hetsron L, Menoukeu-Pamen Olivier, Asamoah Joshua Kiddy K, Jin Zhen. Global stability dynamics and sensitivity assessment of COVID-19 with timely-delayed diagnosis in Ghana. *Comput Math Biophys.* 2022;10(1):87–104.
18. Acheampong Edward, Okyere Eric, Iddi Samuel, Bonney Joseph HK, Asamoah Joshua Kiddy K, Wattis Jonathan AD, Gomes Rachel L. Mathematical modelling of earlier stages of COVID-19 transmission dynamics in Ghana. *Results Phys.* 2022;34:105193.
19. Akindeinde Saheed O, Okyere Eric, Adewumi Adebayo O, Lebelo Ramoshweu S, Fabelurin Olanrewaju O, Moore Stephen E. Caputo fractional-order SEIRP model for COVID-19 Pandemic. *Alex Eng J.* 2022;61(1):829–845.
20. Wu Joseph T, Leung Kathy, Bushman Mary, Kishore Nishant, Niehus Rene, de Salazar Pablo M, Cowling Benjamin J, Lipsitch Marc, Leung Gabriel M. Estimating clinical severity of COVID-19 from the transmission dynamics in Wuhan, China. *Nat Med.* 2020;26(4):506–510.
21. Hellewell Joel, Abbott Sam, Gimma Amy, Bosse Nikos I, Jarvis Christopher I, Russell Timothy W, Munday James D, Kucharski Adam J, Edmunds W John, Funk Sebastian, Eggo Rosalind M, Sun Fiona, Flasche Stefan, Quilty Billy J, Davies Nicholas, Liu Yang, Clifford Samuel, Klepac Petra, Jit Mark, Diamond Charlie, Gibbs Hamish, van Zandvoort Kevin. Feasibility of controlling COVID-19 outbreaks by isolation of cases and contacts. *Lancet Glob Health.* 2020;8(4):e488–e496.
22. Kucharski Adam J, Russell Timothy W, Diamond Charlie, Liu Yang, Edmunds John, Funk Sebastian, Eggo Rosalind M, Sun Fiona, Jit Mark, Munday James D, Davies Nicholas, Gimma Amy, van Zandvoort Kevin, Gibbs Hamish, Hellewell Joel, Jarvis Christopher I, Clifford Sam, Quilty Billy J, Bosse Nikos I, Abbott Sam, Klepac Petra, Flasche Stefan. Early dynamics of transmission and control of COVID-19: a mathematical modelling study. *Lancet Infect Dis.* 2020;20(5):553–558.
23. Contreras Sebastián, Villavicencio H Andrés, Medina-Ortiz David, Biron-Lattes Juan Pablo, Olivera-Nappa Álvaro. A multi-group SEIRA model for the spread of COVID-19 among heterogeneous populations. *Chaos Solitons Fractals.* 2020;136:109925.
24. Gaff Holly, Schaefer Elsa. Optimal control applied to vaccination and treatment strategies for various epidemiological models. *Math Biosci Eng.* 2009;6(3):469–492.
25. Sweilam NH, Al-Mekhlafi SM. Optimal control for a nonlinear mathematical model of tumor under immune suppression: A numerical approach. *Optim Control Appl Methods.* 2018;39(5):1581–1596.

26. Sweilam NH, AL-Mekhlafi SM, Baleanu D. Optimal control for a fractional tuberculosis infection model including the impact of diabetes and resistant strains. *J Adv Res.* 2019;17:125–137.
27. Ball Frank G, Knock Edward S, O'Neill Philip D. Control of emerging infectious diseases using responsive imperfect vaccination and isolation. *Math Biosci.* 2008;216(1):100–113.
28. Ahmed MMEI-Dessoky, Khan Muhammad Altaf. Modeling and analysis of the polluted lakes system with various fractional approaches. *Chaos Solitons Fractals.* 2020;134:109720.
29. Laarabi Hassan, Abta Abdelhadi, Hattaf Khalid. Optimal control of a delayed SIRS epidemic model with vaccination and treatment. *Acta Biotheor.* 2015;63(2):87–97.
30. Hattaf Khalid, Yousfi Noura. Optimal control of a delayed HIV infection model with immune response using an efficient numerical method. *ISRN Biomath.* 2012;2012:1–7.
31. Aldila Dipo, Götz Thomas, Soewono Edy. An optimal control problem arising from a dengue disease transmission model. *Math Biosci.* 2013;242(1):9–16.
32. Ruan Shigui, Xiao Dongmei, Beier John C. On the delayed ross–macdonald model for malaria transmission. *Bull Math Biol.* 2008;70(4):1098–1114.
33. Abta Abdelhadi, Laarabi Hassan, Alaoui Hamad Talibi. The hopf bifurcation analysis and optimal control of a delayed SIR epidemic model. *Int J Anal.* 2014;2014:1–10.
34. Sene Ndolane. SIR epidemic model with Mittag-Leffler fractional derivative. *Chaos Solitons Fractals.* 2020;137:109833.
35. Zaman Gul, Kang Yong Han, Jung Il Hyo. Optimal treatment of an SIR epidemic model with time delay. *Biosystems.* 2009;98(1):43–50.
36. El-Shahed Moustafa, Alsaedi Ahmed. The fractional SIRC model and influenza a. *Math Probl Eng.* 2011;2011:1–9.
37. Ameen I, Baleanu Dumitru, Ali Hegagi Mohamed. An efficient algorithm for solving the fractional optimal control of SIRV epidemic model with a combination of vaccination and treatment. *Chaos Solitons Fractals.* 2020;137:109892.
38. Ali Nasir, Nawaz Rashid, Zada Laiq, Mouldi Abir, Bouzgarrou Souhail Mohamed, Sene Ndolane. Analytical approximate solution of the fractional order biological population model by using natural transform. In: Gul Taza, ed. *J Nanomater.* 2022;2022:1–12.
39. Podlubny Igor. *Fractional Differential Equations: an Introduction to Fractional Derivatives, Fractional Differential Equations, to Methods of Their Solution and Some of Their Applications.* Elsevier; 1998.
40. Lin Wei. Global existence theory and chaos control of fractional differential equations. *J Math Anal Appl.* 2007;332(1):709–726.
41. Silva Cristiana J, Torres Delfim FM. Stability of a fractional HIV/AIDS model. *Math Comput Simulation.* 2019;164:180–190.
42. Ahmed E, Elgazzar AS. On fractional order differential equations model for nonlocal epidemics. *Phys A.* 2007;379(2):607–614.
43. Odibat Zaid M, Shawagfeh Nabil T. Generalized Taylor's formula. *Appl Math Comput.* 2007;186(1):286–293.
44. van den Driessche P, Watmough James. Reproduction numbers and sub-threshold endemic equilibria for compartmental models of disease transmission. *Math Biosci.* 2002;180(1–2):29–48.
45. Fulford GR, Roberts MG, Heesterbeek JAP. The metapopulation dynamics of an infectious disease: Tuberculosis in possums. *Theor Popul Biol.* 2002;61(1):15–29.
46. Kar TK, Nandi Swapna Kumar, Jana Soovoojeet, Mandal Manotosh. Stability and bifurcation analysis of an epidemic model with the effect of media. *Chaos Solitons Fractals.* 2019;120:188–199.
47. Chitnis Nakul, Hyman James M, Cushing Jim M. Determining important parameters in the spread of malaria through the sensitivity analysis of a mathematical model. *Bull Math Biol.* 2008;70(5):1272–1296.
48. Erturk Vedat Suat, Momani Shaher, Odibat Zaid. Application of generalized differential transform method to multi-order fractional differential equations. *Commun Nonlinear Sci Numer Simul.* 2008;13(8):1642–1654.
49. Momani Shaher, Odibat Zaid. Numerical comparison of methods for solving linear differential equations of fractional order. *Chaos Solitons Fractals.* 2007;31(5):1248–1255.
50. Bayrak Mine Aylin, Demir Ali. A new approach for space-time fractional partial differential equations by residual power series method. *Appl Math Comput.* 2018;336:215–230.
51. Martin Olga. Stability approach to the fractional variational iteration method used for the dynamic analysis of viscoelastic beams. *J Comput Appl Math.* 2019;346:261–276.
52. Jong KumSong, Choi HuiChol, Jang KyongJun, Pak SunAe. A new approach for solving one-dimensional fractional boundary value problems via Haar wavelet collocation method. *Appl Numer Math.* 2021;160:313–330.
53. Khudair Ayad R, Haddad SAM, khalaif Sanaa L. Restricted fractional differential transform for solving irrational order fractional differential equations. *Chaos Solitons Fractals.* 2017;101:81–85.
54. Chouhan Devendra, Mishra Vinod, Srivastava HM. Bernoulli wavelet method for numerical solution of anomalous infiltration and diffusion modeling by nonlinear fractional differential equations of variable order. *Res Appl Math.* 2021;10:100146.
55. Diethelm Kai, Ford Neville J, Freed Alan D. Detailed error analysis for a fractional adams method. *Numer Algorithms.* 2004;36(1):31–52.
56. Sweilam Nasser Hassan, El-Sayed Adel Abd Elaziz, Boulaaras Salah. Fractional-order advection-dispersion problem solution via the spectral collocation method and the non-standard finite difference technique. *Chaos Solitons Fractals.* 2021;144:110736.
57. Khudair Ayad R. On solving non-homogeneous fractional differential equations of Euler type. *Comput Appl Math.* 2013;32(3):577–584.
58. Khalaf Sanaa L, Khudair Ayad R. Particular solution of linear sequential fractional differential equation with constant coefficients by inverse fractional differential operators. *Differ Equ Dyn Syst.* 2017;25(3):373–383.
59. Huseynov Ismail T, Mahmudov Nazim I. Delayed analogue of three-parameter Mittag-Leffler functions and their applications to Caputo-type fractional time delay differential equations. *Math Methods Appl Sci.* 2020.
60. Huseynov Ismail T, Ahmadova Arzu, Fernandez Arran, Mahmudov Nazim I. Explicit analytical solutions of incommensurate fractional differential equation systems. *Appl Math Comput.* 2021;390:125590.
61. Ahmadova Arzu, Huseynov Ismail T, Fernandez Arran, Mahmudov Nazim I. Trivariate Mittag-Leffler functions used to solve multi-order systems of fractional differential equations. *Commun Nonlinear Sci Numer Simul.* 2021;97:105735.
62. Huseynov Ismail T, Mahmudov Nazim I. A class of langevin time-delay differential equations with general fractional orders and their applications to vibration theory. *J King Saud Univ - Sci.* 2021;33(8):101596.
63. Ahmadova Arzu, Mahmudov Nazim I. Langevin differential equations with general fractional orders and their applications to electric circuit theory. *J Comput Appl Math.* 2021;388:113299.
64. Jalil Ahmed F Abdel, Khudair Ayad R. Toward solving fractional differential equations via solving ordinary differential equations. *Comput Appl Math.* 2022;41.
65. Mandal Manotosh, Jana Soovoojeet, Nandi Swapna Kumar, Khatua Anupam, Adak Sayani, Kar TK. A model based study on the dynamics of COVID-19: Prediction and control. *Chaos Solitons Fractals.* 2020;136:109889.